ChemPubSoc Europe

DOI: 10.1002/chem.201805421

CHEMISTRY A European Journal Full Paper

Ylides

Isolation of the Metalated Ylides [Ph_3P–C–CN]M (M = Li, Na, K): Influence of the Metal Ion on the Structure and Bonding Situation

Christopher Schwarz[+],[a] Lennart T. Scharf[+],[a] Thorsten Scherpf,[a] Julia Weismann,[b] and Viktoria H. Gessner*[a]

Abstract: The isolation and structural characterization of the cyanido-substituted metalated ylides [Ph_3P–C–CN]M (**1-M**; M = Li, Na, K) are reported with lithium, sodium, and potassium as metal cations. In the solid-state, most different aggregates could be determined depending on the metal and additional Lewis bases. The crown-ether complexes of sodium (**1-Na**) and potassium (**1-K**) exhibited different structures, with sodium preferring coordination to the nitrogen end, whereas potassium binds in an unusual η^2-coordination mode to the two central carbon atoms. The formation of the yldiide was accompanied by structural changes leading to shorter C–C and longer C–N bonds. This could be attributed to the delocalization of the free electron pairs at the carbon atom into the antibonding orbitals of the CN moiety, which was confirmed by IR spectroscopy and computational studies. Detailed density functional theory calculations show that the changes in the structure and the bonding situation were most pronounced in the lithium compounds due to the higher covalency.

Introduction

Bisylidic compounds such as carbodiphosphoranes (CDP) and carbodicarbenes (CDC), have gained intense research interest over the past years.[1] Due to their unique electronic structures, these compounds have been used as strong donor ligands in different research areas, such as for the coordination and stabilization of small and/or reactive molecules[2] or in the preparation of catalytically active transition-metal complexes.[3] The electronic structure itself has been the subject of most controversial discussions.[4] Although initial debates on contributions of the double bonded ylene ($R_3P{=}CR_2$) and the ylidic ionic structures have ended in favor of the ylide description (R_3P^+–C^-R_2), recent computational studies argued for a predominant contribution of a dative-bonding situation ($R_3P{\rightarrow}CR_2$).[5] This captodative bonding mode led to the conclusion that the carbon atom in ylidic compounds can serve as a "central atom" similar to a metal in a complex, which also led to the denotation of bisylides and related compounds as carbones with the carbon atom in the zero oxidation state (Figure 1).[6]

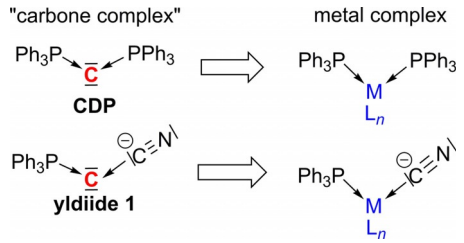

Figure 1. The metallic nature of carbon in ylidic compounds.

Our group has reported on the anionic congeners of bisylidic compounds, that is, α-metalated ylides (yldiides).[7] These compounds also exhibit two lone pairs of electrons at the central ylidic carbon atom and are thus strong donor ligands, which, for example, allowed the stabilization of a series of borenium ions or the synthesis of highly electron-rich phosphine ligands.[8,9] Despite their huge synthetic potential, very little is known about their electronic structures. Only four yldiides have been isolated and structurally authenticated so far.[8,10] In this regard, yldiide **1** seemed to be especially interesting because it can be viewed as an anionic carbone, in which the carbon atom is coordinated like a metal in a cyanido-phosphine complex (Figure 1). Thus, comparable to bisylides, the yldiide may exhibit different bonding situations, which also may be influenced by the counter cation (typically M^+ with M = Li, Na, or K). Therefore, cation coordination in **1-M** can either occur at the cyanido nitrogen or at the α-carbon

[a] C. Schwarz,[+] L. T. Scharf,[+] T. Scherpf, Prof. Dr. V. H. Gessner
Chair of Inorganic Chemistry II, Faculty of Chemistry and Biochemistry
Ruhr University Bochum, Universitätsstrasse 150, 44801 Bochum (Germany)
E-mail: viktoria.gessner@rub.de
Homepage: http://www.ruhr-uni-bochum.de/ac2/

[b] Dr. J. Weismann
Institut für Anorganische Chemie, Julius-Maximilians-Universität Würzburg
Am Hubland, 97074 Würzburg (Germany)

[+] These authors contributed equally to this work.

Supporting information and the ORCID identification number(s) for the author(s) of this article can be found under: https://doi.org/10.1002/chem.201805421.

atom. These different coordination modes have been shown to influence the reactivity of various metalated nitriles[11,12] and are expected to affect the bonding situation.

Comparable to CDPs, the electronic structure in yldiides can be described by different bonding situations. In the past, the ylidic form **1A** (Figure 2) was used to account for the two lone

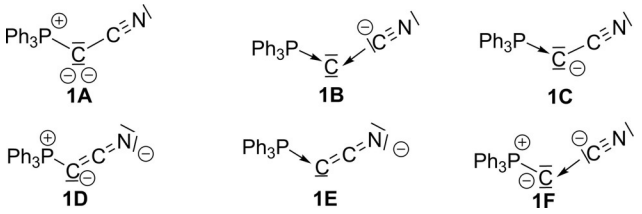

Figure 2. Possible Lewis structures for yldiide **1**.

pairs at the central carbon atom and the high nucleophilicity, which have both been experimentally proven by the use in double-functionalization and cascade reactions or in the formation of digold complexes.[13,14] However, the dative fragmentation pattern **1B** has also been proposed in analogy to transition-metal complexes.[15] Previous DFT studies have already revealed that often different (also unsymmetrical) structures must be considered to fully describe the electronic distribution in metalated ylides.[16,17] Yet, no influence of the metal ion has been considered to date. For example, yldiide **1** can potentially be described by either of the six Lewis structures shown in Figure 2, in which additionally the metal cation can coordinate to either the nitrogen or the carbon atom (hence, 12 structures in total). Thus, to obtain initial insights into the structure and bonding situation of **1**, we set out to isolate and structurally characterize different metal complexes of the yldiide. We were particularly interested in answering the following questions: i) Which kind of structures are formed with different metal cations? ii) Does the bonding situation change with different metals and the different coordination modes of the metal (N- vs. C-coordination)? iii) Do changes in the bonding situation correlate with experimental data (bond lengths, C–N stretching frequencies)?

Results and Discussion

Synthesis and NMR and IR spectroscopic studies

As a starting point of our investigations, we first addressed the isolation of yldiide **1** complexed to different alkali metal cations. The metalated ylide **1-Na** was already reported by Bestmann and co-workers and was used in situ in a variety of organic transformations.[13] The yldiide is readily accessible by a stepwise deprotonation procedure. At first, ylide **1-H** is obtained in high yields by deprotonation of the phosphonium salt **1-H$_2$** with one equiv of sodium hydride or *n*-butyllithium in THF at room temperature (Scheme 1). The use of the lithium base always resulted in the formation of a lithium bromide adduct of **1-H**, in which the lithium is coordinated by the nitrile moiety (see the Supporting Information for XRD analyses

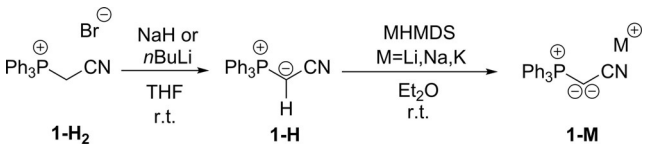

Scheme 1. Preparation of the metalated ylides **1-M** (M = Li, Na, K) from phosphonium salt **1-H$_2$**.

of **1-H$_2$** and **1-H**), whereas in contrast, the sodium base gave way to the "free" ylide **1-H**.

Deprotonation of the ylide **1-H** was performed using alkali metal hexamethyldisilazide (HMDS) bases. Although complete conversion from **1-H** to **1-M** (with M = Li, Na or K) was accomplished with all HMDS bases according to the NMR spectroscopic data (directly obtained after mixing the reagents), only the potassium salt could be isolated in a pure form. For the lithium and sodium yldiides, incorporation of LiHMDS and NaHMDS, respectively, into the structures of **1-M** (see below) excluded their complete removal from the yldiide, and thus complicated the isolation of the pure compounds. This is particularly true for **1-Li**·LiHMDS, which could be isolated only in very low yield (9%). The isolation of **1-Na**·NaHMDS was found to be slightly easier, but it gave strongly varying yields with the best result providing 77% of the product. In contrast, pure **1-K** was obtained as a yellow solid in 84% yield by simple washing of the formed solid with diethyl ether. Overall, the metalated ylides are highly reactive compounds independent of the metal cations or the use of further coordinating ligands. They tend to get easily protonated to **1-H**, particularly in THF and other ethereal solvents, which also complicated spectroscopic studies in solution.[18]

NMR spectroscopic studies were performed on the isolated metaled ylides, both with and without the addition of crown ethers. Only the crown-ether complex of **1-Li** was examined after in situ preparation because its isolation proved to be particularly difficult. The successful formation of the yldiides was confirmed by a distinct high-field shift of the signal in the $^{31}P\{^1H\}$ NMR spectrum from $\delta = 23.2$ ppm for **1-H** to $\delta = -1.9$ to -19.9 ppm for **1-M** (see Table 1). Such a high-field shift has also previously been observed for the formation of other yldiides.[7] Most interestingly, the extent of the high-field shift was found to be dependent on the nature of the metal cation and on the presence of additional donor bases, particularly crown

Table 1. NMR and IR spectroscopic properties of the metalated ylides **1-M** and their corresponding protonated congeners [**1-H$_2$**]**Br** and **1-H** (12c4 = 12-crown-4; 15c5 = 15-crown-5; 18c6 = 18-crown-6).

	δ_P [ppm]	δ_{C1} [ppm] $^1J_{PC}$ [Hz]	δ_{C2} [ppm] $^2J_{PC}$ [Hz]	$\tilde{\nu}$ (CN) (THF) [cm^{-1}]
[**1-H$_2$**]**Br**	21.9	17.8; 54.8	112.2; 9.4	–
1-H	23.2	−2.9; 135	124.7; 7.5	2157
1-Li·(LiHMDS)	−1.9	−3.4 (br)	134.4; 20.1	1989
1-Li·(12c4)	−3.1	−2.6; 131.8	134.6; 12.6	1995
1-Na·(NaHMDS)	−5.2	−5.4; 68.2	142.5; 12.6	2008
1-Na·(15c5)	−10.9	−0.7; 72.7	141.1; 15.6	2023
1-K	−10.5	0.83; 68.0	140.9; 14.4	2001
1-K·(18c6)	−19.9	5.4; 59.2	137.3; 15.6	2014

ethers, thus suggesting an influence of the metal on the electronics of the yldiide. This feature can be impressively seen through the more pronounced high-field shift in the series Li < Na < K, as well as through the further shift upon crown-ether addition to **1-K** [e.g., $\delta(^{31}P) = -10.5$ ppm for **1-K** and -19.9 ppm for **1-K**·(18-crown-6)].

It must be noted that, in contrast to all other complexes, the NaHMDS-containing sodium salt **1-Na** exhibited only a broad signal in the $^{31}P\{^{1}H\}$ NMR spectrum at room temperature. This signal somewhat sharpened upon heating up to 60 °C, and, most interestingly, gave rise to a splitting into four sharp signals at -30 °C. This observation indicates the formation of a complex, in which the yldiides possess four different environments. Exchange on the NMR timescale between these different environments is fast at higher temperatures, whereas it is slow at -30 °C. Four different phosphorus sites were also found in the crystal structure (see below, Figure 3), thus suggesting that the structures are the same both in the solid state as well as in solution.

In addition to the changes of the $^{31}P\{^{1}H\}$ NMR shift, the decrease in the $^{1}J_{PC}$ coupling constant in **1-M** (59–72 Hz) compared to ylide **1-H** (135 Hz) was characteristic of the successful α-metalation. This decrease can be explained by the higher p-character of the P–C linkage due to the increase of s-electron density at the ylidic carbon atom to stabilize the two lone pairs of electrons.[19]

The ^{13}C NMR shift of the nitrile carbon atom proved to be most indicative to distinguish between N- versus C-metalation in α-metalated nitriles, because the chemical shift is highly sensitive to the local environment.[20] Typically, N-metalated nitriles show signals between $\delta(^{13}C) = 140$ and 157 ppm, whereas the carbon in the corresponding C-metalated nitriles resonates at higher field between $\delta(^{13}C) = 115$ and 138 ppm.[21] Yet, comparison of the ^{13}C NMR shifts of the different metal salts of **1** and their crown-ether complexes shows no clear evidence for either coordination mode (Table 1). All shifts are approximately in between the two ranges, thus suggesting either a different or both types of coordination in solution.

IR spectroscopy of the different yldiides **1-M** in THF solution proved to be highly informative. The C–N stretching frequencies decrease considerably upon each deprotonation step from $\tilde{\nu} = 2250$ cm^{-1} in **1-H$_2$** to 2137 cm^{-1} in **1-H** and approximately 2000 cm^{-1} in **1-M**. This clearly indicates a decrease in the C–N bond order and a transition from a C–N triple to a double bond.[22] Considering the different possible Lewis structures of **1-M**, this observation can only be explained by structures with a covalent C=C double bond (**1D** or **1E**, Figure 2) or by the captodative bonding mode (**1B** or **1F**) with strong π back-donation from the central carbon atom into the CN moiety (analogous to an electron-rich metal in CO complexes). Two further interesting observations can be made from the IR data provided in Table 1 with respect to the impact of metal coordination on the structure of **1-M**: i) The CN stretching frequency is significantly lower for the lithium compounds **1-Li** and **1-Li**·(12c4) compared to their sodium and potassium analogues and ii) the crown-ether complexes exhibit higher frequencies (approx. 10–15 cm^{-1}) than their crown-ether-free analogues. These observations correlate with the increase in the electropositive character of the metal and the decrease of covalent character in their bonds to other elements. It seems that the more tightly the metal is bound to the yldiide the weaker is the C–N bond and thus, it is the weakest for **1-Li** (see below). A similar observation has also been reported for metalated and polymetalated nitriles.[23]

Crystallographic studies

To gain further insights into the structures of **1-M**, crystallization of the different metal salts, including their crown-ether complexes, was attempted. Although all attempts to crystallize pure **1-K** failed, the NaHMDS/LiHMDS-containing sodium and lithium compounds could be crystallized by diffusion of *n*-hexane into a benzene solution of **1-Na** and by storage of an *n*-hexane solution of **1-Li**, respectively. The structure of the sodium compound was only of poor quality due to the presence of highly disordered solvent molecules in the structure, impeding a detailed discussion of the structure parameters (see the Supporting Information for details). Nonetheless, it unambiguously confirms the coordination of two NaHMDS to eight molecules of **1-Na**, which are arranged in an unusual, non-symmetrical fashion. In [(**1-Na**)$_8$(NaHMDS)$_2$], the sodium atoms feature contacts to the ylidic carbon atom as well as to the cyanido nitrogen atom, in accordance with the ^{13}C NMR shift of C1 lying between the typical shifts for C- and N-coordination (see above). The same holds true for the analogous lithium compound, which forms an unsymmetrical aggregate of the composition [(**1-Li**)$_3$(LiHMDS)$_5$] in the solid state. The molecular structure is shown in Figure 3 and structural details are given in Table 2 and the Supporting Information. The aggregate is formed by two parts consisting of one yldiide **1-Li** and two LiHMDS molecules, which are connected by a further molecule of **1-Li** and LiHMDS. A possible C_S-symmetry of the compound is broken solely by the orientation of the yldiide in the central unit (highlighted in blue in Figure 3). In addition to the structures of the lithium and sodium complexes of **1**, a series of different LiHMDS and NaHMDS structures with varying geometries and aggregation motifs has been reported in the literature.[24]

A comparison of structural parameters of the central PCCN moiety in the series of compounds **1-H$_2$**, **1-H** and **1-Na**·(HMDS) and [(**1-Li**)$_3$(LiHMDS)$_5$] shows that the P–C and the C1–C2 bond shorten after each deprotonation step, the P–C bond goes from 1.811(2) Å to about 1.68 Å and the C–C bond from 1.45 to 1.35 Å, thus in line with a transition from a single to a double bond. In contrast, the C–N bond length increases from 1.136(2) Å in **1-H$_2$** to about 1.18 Å in the lithium compound[(**1-Li**)$_3$(LiHMDS)$_5$], which is consistent with a reduction of the C–N bond order and an C=C=N structure. The P-C1-C2 and C1-C2-N angles change only slightly compared to the ylide, however, it is noticeable that the C-C-N linkage clearly deviates from linearity.

To further analyze the oligomeric structures and to probe whether the different alkali metals exhibit any preference for coordination to the nitrogen-end or the ylidic carbon atom,

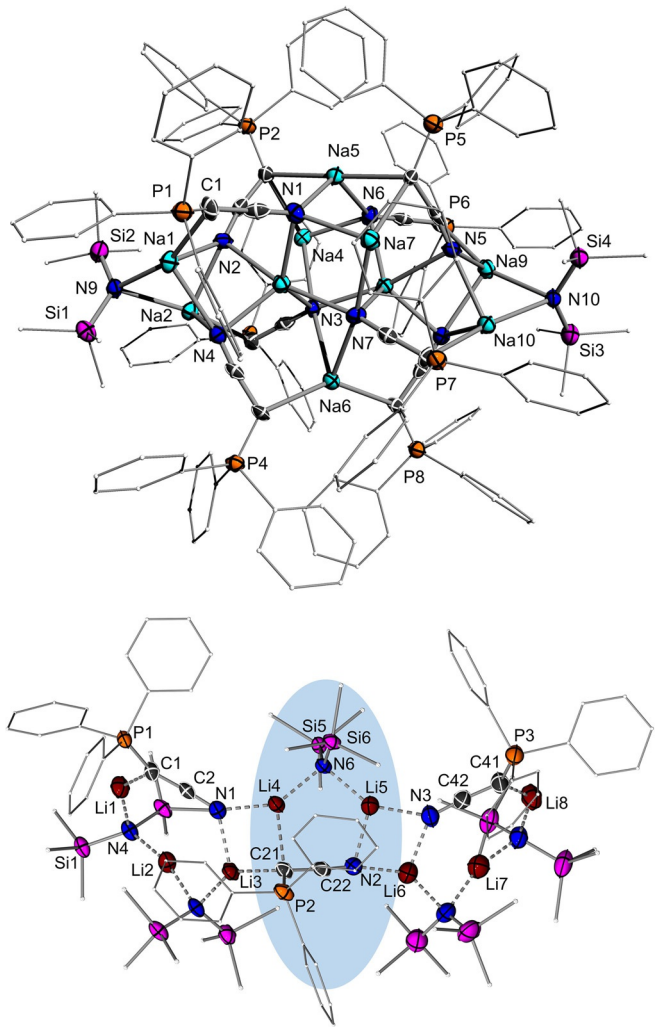

Figure 3. Molecular structures of [(**1-Na**)$_8$(NaHMDS$_2$)] and [(**1-Li**)$_3$(LiHMDS)$_5$] in the solid state. Hydrogen atoms are omitted for clarity; displacement parameters drawn at the 30% (for [(**1-Na**)$_8$(NaHMDS$_2$)]) and 50% probability level (for [(**1-Li**)$_3$(LiHMDS)$_5$]). Selected bond lengths and angles are given in Table 2 and structural details in the Supporting Information.

Table 2. Comparison of structural properties of the metalated ylides **1-M** and their corresponding protonated congeners [**1-H$_2$**]**Br** and **1-H**; bond lengths are given in Å, angles in °; for **1-K**·(**18c6**), average values of two crystallographically independent molecules in the asymmetric unit are given.

	P–C	C–C	C–N	P-C-C	C-C-N
[**1-H$_2$**]Br	1.811(2)	1.453(2)	1.136(2)	112.1(1)	179.1(2)
1-H	1.693(2)	1.388(3)	1.153(3)	123.0(2)	178.4(3)
1-H·LiBr	1.704(2)	1.388(3)	1.158(3)	120.9(2)	178.2(2)
[(**1-Li**)$_3$(LiHMDS)$_5$]	1.666(2)	1.344(3)	1.188(2)	128.5(1)	172.7(2)
	1.691(2)	1.358(3)	1.181(3)	113.7(1)	174.6(2)
	1.681(2)	1.349(3)	1.183(3)	121.8(2)	174.3(2)
[[(**1-Li**)$_4$·(18c6)]$_\infty$	1.654(3)	1.344(3)	1.188(3)	121.9(2)	173.7(3)
	1.642(3)	1.342(4)	1.171(3)	131.2(3)	171.9(3)
[**1-Na**·(15c5)]	1.637(3)	1.370(5)	1.167(4)	125.3(3)	174.1(3)
[**1-K**·(18c6)]	1.650(2)	1.377(3)	1.179(3)	120.9(2)	173.7(3)

crown ethers were added to **1-M** for additional complexation of the metal. Unfortunately, crystallization attempts with the small 12-crown-4 repeatedly failed for the lithium compound. However, single crystals were obtained with both 18-crown-6 (18c6) and 15-crown-5 (15c5) (Figure 4).[25] Compound [(**1-Li**)$_3$·(15c5)]$_2$ forms a unique C_i-symmetric dimeric structure consisting of six yldiides and two crown ethers. The central structural motif is formed by a (Li–C–C–N)$_2$ eight-membered ring connected to two Li_2N_2 four-membered rings. Due to the large size of 15-crown-5, the crown ether serves as a bridging ligand for coordinating the two lithium cations. In the solid state, all yldiides exhibit contacts of the metal to both the ylidic carbon atom and the nitrogen of the nitrile moiety. In contrast to [(**1-Li**)$_3$·(15c5)]$_2$, the 18-crown-6 compound of **1-Li**, [(**1-Li**)$_4$·(18c6)]$_\infty$, exhibits a polymeric structure consisting of two different dimeric subunits that contain a Li_2N_2 four-membered ring. In one of these units the lithium atoms are coordinated solely by the nitrile moiety and the crown ether, whereas they also bind

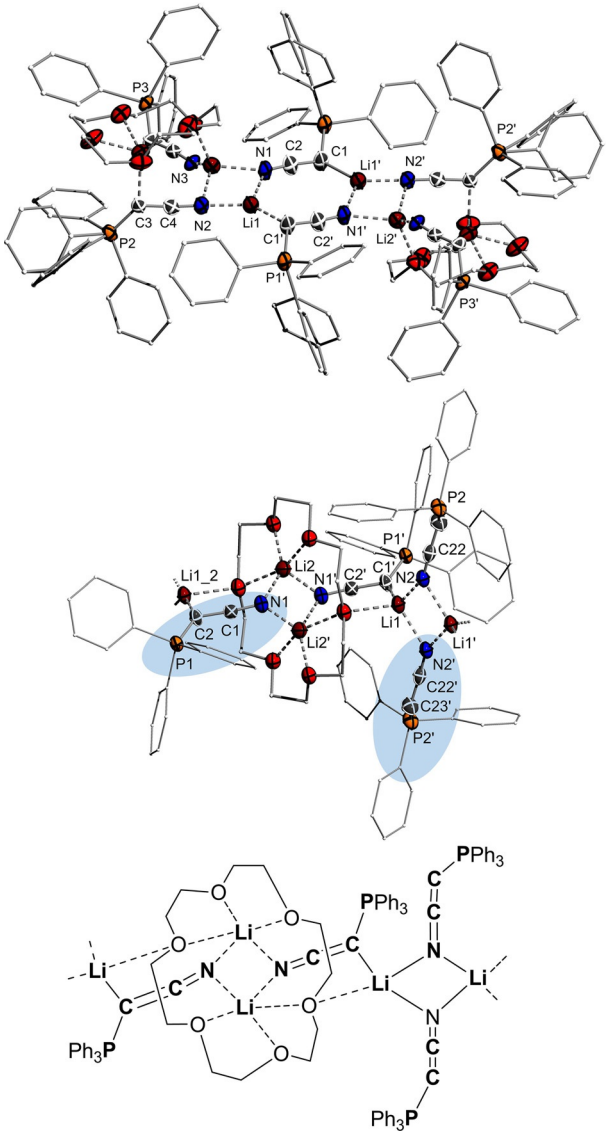

Figure 4. (Top) Molecular structure of [(**1-Li**)$_3$·(15c5)]$_2$ and (middle) [(**1-Li**)$_4$·(18c6)]$_\infty$ in the solid state. Hydrogen atoms and solvent molecules are omitted for clarity; 50% (30% for [(**1-Li**)$_3$·(15c5)]$_2$ displacement parameters. Selected bond lengths and angles are given in Table 2.[25]

to the ylidic carbon atom in the second fragment. Thus, one of the yldiides again features mixed C/N-coordination of the metal, whereas the other only binds the metal at the nitrogen end (the different coordination environments are highlighted in blue in Figure 4). This results in significant structural differences in these two yldiides. As such, the exclusively N-coordinated yldiide features a significantly shorter C–N bond (1.171(3) versus 1.188(3) Å) and a wider P-C-C angle (131.2(3) and 121.9(2)°) compared to its C,N-complexed analogue (see explanation below).

The crown ether complexes of **1-Na** and **1-K** were obtained by diffusion of *n*-hexane into a solution of **1-Na** in toluene and *n*-pentane into a THF solution of **1-K**, respectively. In contrast to **1-Li**, the 15-crown-5 and 18-crown-6 complexed sodium and potassium compounds, respectively, exhibit monomeric structures (Figure 5). Yet, they differ in the coordination of the

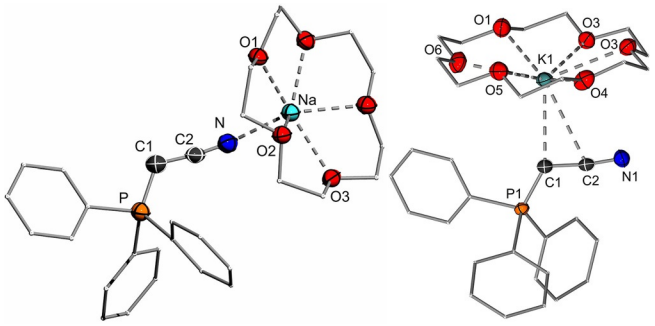

Figure 5. (a) Molecular structure of [**1**-**Na**·(15c5)] and [**1**-**K**·(18c6)] in the solid state. [**1**-**K**·(18c6)] crystallizes with two crystallographically independent molecules in the asymmetric unit, only one of which is shown here. Hydrogen atoms and THF solvent molecules are omitted for clarity; 50% displacement parameters. Selected bond lengths and angles are given in Table 2.

yldiide to the respective metal cation. Although the harder sodium atom coordinates solely to the nitrogen atom of the nitrile, the softer potassium prefers the interaction with the ylidic and nitrile carbon atom. To the best of our knowledge, such a η^2-coordination mode has never been observed for any other α-metalated nitrile. Until now, only C- or N-metalation have been observed, in which the alkali metals usually prefer N-coordination.[26] The K–C bond lengths vary between 2.899(2) and 3.293(2) Å and are in the range of known organopotassium compounds (bond lengths correspond to both independent molecules in the asymmetric unit).[27] Despite the slightly bent C-C-N linkage (173.7(3)°), the K–N distance amounts to 3.749(2) Å and is thus longer than typical K–N bond lengths (2.77–3.04 Å).[27c,28] However, in contrast to transition-metal olefin complexes, the nitrogen atom in the structure of **1-K**·(18c6) points towards the metal center suggesting that nonetheless some weaker K–N interaction might be present in the complex.

With respect to the bonding situation, the η^2-coordination is well in line with the IR data and further confirms the change in the bonding situation from a single to a double bond in **1-K** compared with the phosphonium salt. This assumption is further supported by the structural changes in the yldiides, that is, the shortening of the P–C and C1–C2 bond as well as the lengthening of the C–N bond. Hence, the crystal structures further argue for the predominance of the bonding situation C=C=N.

Overall, the solid-state structures show that the coordination modes in **1-M** are rather complex and diverse and strongly depend on the metal and additional Lewis bases. Both N- and C-coordination are observed, although N-coordination seems to be slightly more preferred for the harder cations (see **1-Na**·(15c5) and [(**1-Li**)$_4$·(18c6)]$_\infty$).

Computational studies

To gain insights into the different coordination modes of the alkali metals in yldiide **1-M** and their impact on the electronic distribution, computational studies were performed using monomeric systems (comparable to the structures of **1-K** and **1-Na** with crown ether) and dimethyl ether (Me_2O) for completion of the coordination sphere of the metal. At first, the energetics of C- and N-coordination of the yldiide were calculated for each metal (Li, Na, K), showing that N-coordination in **1-M** is strongly preferred for lithium ($\Delta G = -28.4$ kJ mol^{-1}) and less favored for sodium ($\Delta G = -24.5$ kJ mol^{-1}) and particularly less favored for potassium ($\Delta G = -9.1$ kJ mol^{-1}). This trend is expected according to the HSAB (hard and soft acids and bases) concept. Despite the preference of N-coordination for potassium, the calculations also reflect the preferred coordination of potassium to both carbon atoms of the α-metalated nitrile, as found in the crystal structure (Figure 5). Energy optimizations of geometries with the metal solely bound to the α-carbon atom always resulted in a shift of the metal towards the CN moiety.

Investigation of the two highest occupied molecular orbitals (HOMO) showed that they are essentially independent of the metal coordination. This is expected because of the mostly electrostatic nature of the interactions between the yldiide and the metal cations. Thus, even for the most covalently bound lithium, the Wiberg bond indices (WBI) of the C–Li and N–Li bonds in **1-Li** amount to only 0.06 and 0.08, respectively. In addition, the energy of the orbitals is also unaffected by the alkali metal. Overall, the HOMO and HOMO-1 are mostly undisturbed compared to the "metal-free" yldiide. Both orbitals are distributed over the whole C–C–N linkage thus confirming the delocalization of one of the lone pairs at carbon into the CN substituent (Figure 6, top). This is again well in line with the decrease in the C–N stretching frequency as well as the lengthening of the C–N bond and shortening of the C–C bond upon metalation.

In contrast to the orbitals, the introduction of a metal ion to the free yldiide has a significant impact on the charges in the molecule. As shown by the calculated natural population analysis (NPA) charges in Figure 6b, the lithium atom shifts the charge density towards itself. This can clearly be seen by comparison with the "free" yldiide. Hence, a more negative charge is present at the ylidic carbon atom (−1.07 vs. −1.29) in the case of C-coordination, and similarly the negative charge increases at the nitrogen atom (−0.57 vs. −0.83) upon N-coordi-

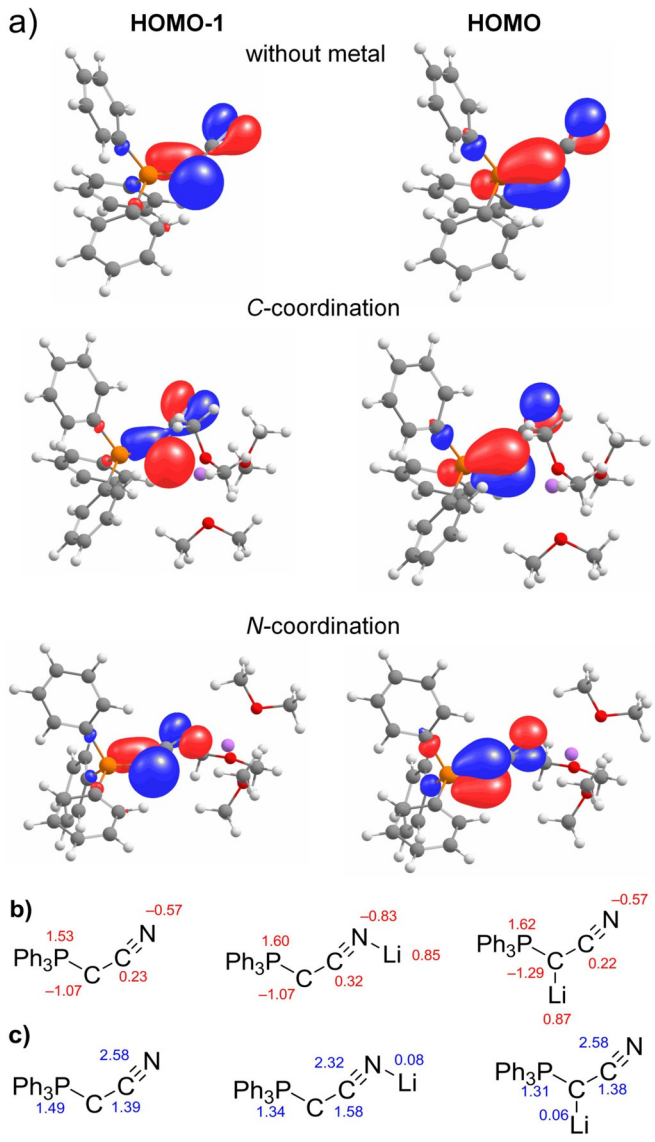

Figure 6. (a) Representations of the HOMO-1 with and without coordination of lithium; (b) NPA charges and (c) WBIs depending on metal coordination.

nation. Interestingly, this charge transfer is most pronounced for lithium. For example, in case of N-metalation, the charge at the nitrogen atom becomes more positive, from −0.83 to −0.78 and −0.75 when going from lithium to sodium and potassium, respectively. This is somewhat counter intuitive to the more electropositive nature of the heavier metals and their higher tendency for ionic bonding. However, the higher covalency of the bonds to lithium results in stronger orbital interactions and thus probably in a more efficient transfer of electron density from the ylidic carbon atom into the π orbitals of the C–N bond. This corroborates the decrease in the WBI of the C–N bond from potassium (WBI(C-N) = 2.41) to lithium (WBI(C-N) = 2.32) (Figure 6c and the Supporting Information) and the particularly low stretching frequencies for the lithium compounds observed in the IR spectra (Table 1).

As a next step, energy decomposition analysis with natural orbitals for chemical valency (EDA-NOCV)[29] calculations for all six different fragmentation patterns were performed including C- and N-coordination of the metal cation (see the Supporting Information). To this end, the yldiide was fragmented once by cleavage of the P–C bond and once by cleavage of the C–C bond to independently evaluate the respective bonding situation. The different types of bonding arise from different types of covalent interactions (captodative, electron-sharing and ylidic) and thus indicate different chemical bonding situations. The importance of each bonding situation was judged based on the orbital energy value (ΔE_{Orb}). The fragmentation with the lowest absolute ΔE_{Orb} value was the best choice for describing the bonding situation in a molecule because the smallest alteration of the electronic charge distribution is required to yield the electronic structure of the molecule.[5b,30]

As shown by the results depicted in Table 3 for the P–C bond, the dative bonding is the energetically most favored bonding situation for the free yldiide and becomes even more

Table 3. EDA-NOCV results for the P–C and the C–C bond (values in kcal mol^{-1}).

	P–C			C–C		
	dative	double	ylidic	dative	double	ylidic
			"free yldiide"			
ΔE_{Pauli}	536	366	555	577	424	415
ΔE_{Elstat}	−266	−228	−476	−251	−211	−217
ΔE_{Orb}	**−353**	**−395**	**−439**	**−459**	**−457**	**−298**
ΔE_{Int}	−83	−256	−359	−133	−244	−100
			N-coordination			
ΔE_{Pauli}	563	336	413	627	462	473
ΔE_{Elstat}	−272	−205	−324	−267	−229	−298
ΔE_{Orb}	**−378**	**−376**	**−380**	**−481**	**−462**	**−442**
ΔE_{Int}	−86	−245	−291	−121	−229	−267
			C-coordination			
ΔE_{Pauli}	416	433	447	497	397	384
ΔE_{Elstat}	−205	−234	−327	−304	−284	−206
ΔE_{Orb}	**−296**	**−384**	**−353**	**−392**	**−421**	**−332**
ΔE_{Int}	−86	−185	−233	−199	−308	−154

favorable when changing from the unmetalated to the C-coordinated form [ΔE_{Orb} = −353 (free) vs. −296 kcal mol^{-1} (C-form)]. In contrast, when the lithium is coordinated to the nitrogen atom, the dative binding mode becomes significantly less favorable [ΔE_{Orb} = −353 (free) vs. −378 kcal mol^{-1} (N-form)]. This is mostly caused by the higher electron density shift from the phosphine lone pair to the empty orbital of the carbon atom upon N-coordination (see the Supporting Information). The changes caused by C- and N-metalation are well in line with the determined NPA charges. As such, C-coordination results in a charge accumulation at the ylidic carbon atom and thus in its reluctance to accept more electron density. This supports a dative interaction because here, less electron density is transferred than for a double bond or an ylidic interaction. Likewise, when the nitrogen atom is coordinated by the lithium atom, the whole fragment becomes more electron-accepting, leading to a more favorable ylidic interaction relative to the dative bonding. The π backbonding is largely unaffected by the different coordination modes (see Supporting Information). Simi-

larly, the double bonded form is unaffected by the different coordination modes.

In contrast to the P–C bond, the C–C bond is clearly ylidic in the non-metalated as well as in the C-metalated form. Analogous to the P–C bond, the dative interaction between the two carbon atoms becomes more favorable when the lithium atom is coordinated by the central carbon atom due to the increased negative charge. This changes drastically in case of N-coordination, for which all bonding situations are almost equal in energy. Most likely, this is also related to the "electron-withdrawing" effect of the lithium atom, rendering the fragment less capable of forming an ylidic bond so that the C=C=N bonding mode becomes equal in energy. The dative interaction is largely unaffected by the N-coordination of the metal. Thus, the EDA calculations suggest that, for C- and N-coordination of the metal, the ylidic bonding situation in the CCN fragment is favorable, but that N-coordination results in a higher preference for the double-bonded structure. This observation is interesting because the calculations also predicted that N-coordination is the most favored for lithium, which therefore should show the highest preference for the $Ph_3P \rightarrow C{=}C{=}N{-}M$ structure and for the weakest C–N bond. This is consistent with the IR data, which showed the lowest C–N stretching frequencies for the lithium compounds, and also with the calculated WBIs. The preferred structures according to the EDA analysis are depicted in Figure 7. Thus, no analogous metal-like behavior of carbon analogous to bisylidic compounds is found here (see Figure 1).

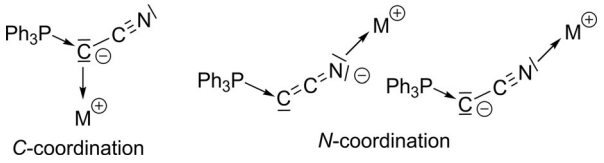

Figure 7. Favored bonding situations depending on the metal coordination.

Altogether, our data show that the bonding situation in metalated ylides depends on the charge distribution in the molecule, which in turn depends on the nature of the metal and on the position where the alkali metal binds to the molecule. Despite the mostly electrostatic nature of the metal interactions (WBI close to zero), higher covalency in the M–X (X = C, N) bonds leads to more pronounced changes than the metal-free system. The fact that the introduction of a cation (or simple cationic charge) has an impact on the bonding situation has also been reported for carbon monoxide, CO.[31] These results suggest that in polar molecules, also other weak interactions, such as those of solvent molecules, may influence the bonding situation. This is particularly true for compounds with large charge accumulations. In fact, this is not surprising because solvent molecules have often changed the reactivity of compounds particularly in polar reagents like alkali or alkaline earth metal compounds.[32] Indeed, the first systematic reactivity studies of the metalated ylides **1-M** with chlorophosphines indicated that the N- versus C-attack of the phosphine strongly depends on the nature of the metal, but also on the solvent [coordinating (THF) versus weakly coordinating (toluene)]. These structure/solvent reactivity relationships are part of ongoing detailed investigations, but clearly indicate that the reactivity of the metalated ylide is complex and strongly influenced by the structure formed under the respective reaction conditions and hence on the resulting changes in the bonding situation.

Conclusions

We have reported a detailed study of the structure and bonding situation of the cyanido-functionalized, metalated ylide [Ph_3P–C–CN]M (**1-M**, M = Li, Na, K). The compounds show a remarkable structural diversity depending on the metal and additional Lewis bases. In the crown-ether-ligated complexes, different monomeric structures were found for sodium and potassium, in which sodium prefers the coordination at the nitrogen of the cyanido group, whereas potassium exhibits an unusual η^2-coordination mode binding to the C–C linkage. IR spectroscopic studies demonstrate that the bonding situation in the CCN linkage changes upon metalation and is influenced by the nature of the metal. The changes are most pronounced for lithium, which exhibits the weakest C–N bond due to its more covalent interaction with the CCN fragment. Calculations on the bonding situation and electronic structure show that coordination of the metal to **1** significantly affects the NPA charges in the molecule. Compared with the metal-free yldiide, the largest charge transfer is found for lithium, which efficiently pulls electron density towards itself. Energy decomposition analyses suggest that the bonding between the ylidic carbon atom and the cyanido group lies between an ylidic and a classical double bond. The latter becomes more important in case of the coordination of the metal at the nitrogen end rather than at the ylidic carbon atom.

Experimental Section

General methods and materials

All experiments were carried out under a dry, oxygen-free argon atmosphere using standard Schlenk techniques. Solvents were dried using an MBraun SPS-800 (THF, toluene, Et_2O, CH_2Cl_2, *n*-pentane, *n*-hexane) or following standard procedures. All chemicals and reagents were purchased from Sigma–Aldrich, ABCR, Rockwood Lithium, or Acros Organics and used without further purification. Compound [**1-H$_2$**]B was prepared in analogy to literature reports.[33]

Preparation of 1-H: Phosphonium salt [**1-H$_2$**]Br (29.0 g, 75.9 mmol, 1 equiv) and sodium hydride (1.91 g, 79.7 mmol, 1.05 equiv) were suspended in THF (250 mL) and stirred for six days. The solvent was removed in vacuo and the remaining solid was extracted with CH_2Cl_2 (4×50 mL). The combined CH_2Cl_2 fractions were layered with 200 mL *n*-pentane. After 3 weeks, colorless crystals formed, which were filtered and dried under vacuum, giving the product as a colorless solid (18.3 g, 60.7 mmol, 80%). Spectroscopic data are in accordance with literature reports.[13]

Preparation of [(1-Li)$_3$(LiHMDS)$_5$]: LiHMDS (1.44 g, 8.61 mmol, 15 equiv) was suspended in toluene (15 mL) and added through a filter cannula to **1-H** (500 mg, 1.67 mmol, 3.0 equiv). After stirring

for 14 h, the solvent was removed in vacuo and *n*-hexane (20 mL) was added. Upon standing for three days, the product precipitated from the solution. The supernatant solvent was removed with a syringe, the remaining solid was subsequently dried in vacuo and gave the product as a colorless solid (91 mg, 51.0 μmol, 9%; 1 equiv). ^{1}H NMR (400.1 MHz, [D$_8$]THF): $\delta = 7.85–7.60$ (m, 18H; C*H*$_{PPh_3}$), 7.49–7.17 (m, 27H; C*H*$_{PPh_3}$), −0.16 ppm (s, 90H; NSi(C*H*$_3$)$_3$); ^{31}P{^{1}H} NMR (162.1 MHz, [D$_8$]THF): $\delta = -1.9$ ppm; ^{13}C{^{1}H} NMR (100.7 MHz, [D$_8$]THF) $\delta = 137.2$ (d, $^1J_{CP} = 92.4$ Hz; $C_{PPh_3,\ ipso}$), 134.4 (d, $^2J_{CP} = 20.1$ Hz; *C*CN), 133.0 (d, $^2J_{CP} = 9.04$ Hz; *C*H$_{PPh_3,\ ortho}$), 130.3 (s; *C*H$_{PPh_3,\ para}$), 128.4 (d, $^3J_{CP} = 11.0$ Hz; *C*H$_{PPh_3,\ meta}$), 6.0 (s; NSi(*C*H$_3$)$_3$), −3.4 ppm (br; P*C*CN); FT-IR (KBr, in THF): $\tilde{\nu} = 1989$ cm^{-1}.

Preparation of [(1-Na)$_8$(NaHMDS)$_2$]: NaHMDS (0.856 g, 4.67 mmol, 11.2 equiv) was dissolved in toluene (15 mL) and the supernatant solution was added through a filter cannula to **1-H** (1.00 g, 3.32 mmol, 8.0 equiv). After stirring the reaction mixture for 3 h, *n*-hexane (20 mL) was added, resulting in the precipitation of a yellow solid from the solution. The suspension was filtered with a fritted glass funnel and dried under vacuum to give the product as yellow solid (0.945 g, 2.56 mmol, 77%, 1 equiv). Single crystals suitable for X-ray diffraction were obtained by slow diffusion of *n*-hexane into a benzene solution. ^{1}H NMR (250.1 MHz, [D$_8$]THF) $\delta =$ 7.9–7.6 (m, 48H; C*H*$_{PPh_3}$), 7.4–6.8 (m, 72H; C*H*$_{PPh_3}$), −0.2 ppm (s, 36H; NSi(C*H*$_3$)$_3$; ^{31}P{^{1}H} NMR (162.1 MHz, [D$_8$]THF): $\delta = -5.1$ ppm; ^{13}C{^{1}H} NMR (75.5 MHz, [D$_8$]THF) $\delta = 142.5$ (d, $^2J_{CP} = 12.6$ Hz; *C*CN), 137.9 (d, $^1J_{CP} = 84.5$ Hz; $C_{PPh_3,\ ipso}$), 132.9 (d, $^2J_{CP} = 9.1$ Hz; *C*H$_{PPh_3,\ ortho}$), 129.8 (d, $^4J_{CP} = 2.7$ Hz; *C*H$_{PPh_3,\ para}$), 128.3 (d, $^3J_{CP} = 11.1$ Hz; *C*H$_{PPh_3,meta}$), 6.7 (s; NSi(*C*H$_3$)$_3$), −5.4 ppm (d, $^1J_{CP} = 68.2$ Hz; P*C*CN); FT-IR (KBr, in THF): $\tilde{\nu} = 2008$ cm^{-1}.

Preparation of 1-K: Ylide **1-H** (4.00 g, 13.3 mmol, 1 equiv) and KHMDS (2.78 g, 13.9 mmol, 1.05 equiv) were suspended in Et$_2$O (250 mL) and stirred for two days. The suspension was filtered with a glass frit, washed with Et$_2$O (2×10 mL) and dried in vacuum to give the product as yellow solid (3.77 g, 11.1 mmol, 84%; 1 equiv). ^{1}H NMR (400.3 MHz, [D$_8$]THF): $\delta = 7.89–7.56$ (m, C*H*$_{PPh_3}$), 7.33–7.00 ppm (m, 9H; C*H*$_{PPh_3}$); ^{31}P{^{1}H} NMR (162.1 MHz, [D$_8$]THF): $\delta =$ −10.5 ppm. ^{13}C{^{1}H} NMR (100.7 MHz, [D$_8$]THF): $\delta = 140.9$ (d, $^2J_{CP} =$ 14.4 Hz; *C*CN), 138.6 (d, $^1J_{CP} = 83.1$ Hz; $C_{PPh_3,\ ipso}$), 132.8 (d, $^2J_{CP} =$ 8.9 Hz; *C*H$_{PPh_3,\ ortho}$), 129.6 (s; *C*H$_{PPh_3,\ para}$), 128.3 (d, $^3J_{CP} = 10.9$ Hz; *C*H$_{PPh_3,\ meta}$), 0.8 ppm (d, $^1J_{CP} = 68.0$ Hz; P*C*CN); FT-IR (KBr, in THF): $\tilde{\nu} = 2001$ cm^{-1}.

Preparation of [1-Na·(15c5)]: The compound [(**1-Na**)$_8$(NaHMDS)$_2$] (400 mg, 1.08 mmol, 0.13 equiv) and 15-crown-5 (273 mg, 0.246 mL, 1.24 mmol, 1.2 equiv) were suspended in toluene (15 mL). After stirring for 3 h at room temperature, a red solid precipitated from the reaction mixture. The suspension was filtered with a glass frit and the obtained solid was dried under vacuum to give the product as a red solid (340 mg, 0.600 mmol, 55%; 1 equiv). Single crystals suitable for X-ray diffraction were obtained by slow diffusion of *n*-hexane into a toluene solution. ^{1}H NMR (400.3 MHz, [D$_8$]THF) $\delta = 7.94–7.61$ (m, 6H; C*H*$_{PPh_3}$), 7.38–7.04 (m, 9H; C*H*$_{PPh_3}$), 3.56 ppm (s, 24H; C*H*$_2$); ^{31}P{^{1}H} NMR (162.1 MHz, [D$_8$]THF): $\delta = -10.9$ ppm; ^{13}C{^{1}H} NMR (100.7 MHz, [D$_8$]THF): $\delta =$ 141.1 (d, $^2J_{CP} = 15.6$ Hz; *C*CN), 139.1 (d, $^1J_{CP} = 83.0$ Hz; $C_{PPh_3,\ ipso}$), 132.9 (d, $^2J_{CP} = 8.6$ Hz; *C*H$_{PPh_3,\ ortho}$), 129.4 (d, $^2J_{CP} = 2.7$ Hz; *C*H$_{PPh_3,\ para}$), 128.1 (d, $^3J_{CP} = 10.8$ Hz; *C*H$_{PPh_3,\ meta}$), 70.5 (s; *C*H$_{215c5}$), −0.7 ppm (d, $^1J_{CP} = 72.7$ Hz; P*C*CN); FT-IR (KBr, in THF): $\tilde{\nu} = 2023$ cm^{-1}.

Preparation of [1-K·(18c6)]: The compound **1-K** (100 mg, 29.5 μmol, 1 equiv) and 18-crown-6 (93.0 mg, 35.4 μmol, 1.2 equiv) were suspended in THF (2 mL). After stirring for 3 h at room temperature, all solids were completely dissolved. Subsequent addition of *n*-hexane (6 mL) resulted in the precipitation of a yellow solid, which was filtered with a glass frit and dried under vacuum. The product was obtained as a yellow solid (35.1 mg, 58.0 μmol, 20%, 1 equiv). Single crystals suitable for X-ray diffraction were obtained by slow diffusion of *n*-pentane into a THF solution. NMR spectra in the presence of excessive 18-crown-6: ^{1}H NMR (400.1 MHz, [D$_8$]THF) $\delta = 7.85–7.65$ (m, 6H; C*H*$_{PPh_3}$), 7.26–7.11 (m, 9H; C*H*$_{PPh_3}$); ^{31}P{^{1}H} NMR (162.1 MHz, [D$_8$]THF): $\delta = -19.9$ ppm; ^{13}C{^{1}H} NMR (100.7 MHz, [D$_8$]THF): $\delta = 140.6$ (d, $^1J_{CP} = 77.8$ Hz; $C_{PPh_3,\ ipso}$),, 137.3 (d, $^2J_{CP} = 15.6$ Hz; *C*CN), 132.9 (d, $^2J_{CP} = 8.5$ Hz; *C*H$_{PPh_3,\ ortho}$), 128.6 (s; *C*H$_{PPh_3,\ para}$), 127.5 (d, $^3J_{CP} = 10.5$ Hz; *C*H$_{PPh_3,\ meta}$), 5.4 ppm (d, $^1J_{CP} =$ 59.2 Hz; P*C*CN); FT-IR (KBr, in THF): $\tilde{\nu} = 2014$ cm^{-1}.

Single-crystal X-ray diffraction

Data collection of all compounds was conducted either with a Bruker X8-APEX II ([**1-H$_2$**]Br, **1H**·LiBr), STOE-IPDS 2 ([(**1-Na**)$_8$(NaHMDS)$_2$]), Oxford SuperNova (**1-H**, [(**1-Li**)$_3$(LiHMDS)$_5$], [(**1-Li**)$_3$(15c5)]$_2$, [**1-Na**·(15c5)], [**1-K**·18c6]) or Oxford Synergy diffractometer [(**1-Li**)$_4$(18c6)]$_\infty$. Crystals for investigation were coated in an inert oil (perfluoropolyalkyl ether) and mounted on a fiber loop and placed in a cold N_2 stream on the diffractometer. The data were collected using the APEX 2 (Bruker), X-Area (Stoe) or CrysAlisPro (Oxford) software and the crystal structure determinations were accomplished at 100 K using Cu$_{K\alpha}$ radiation ($\lambda = 1.54184$ Å) or Mo$_{K\alpha}$ radiation ($\lambda = 0.71073$ Å). The structures were solved using direct methods, refined with the SHELX software package[34] and expanded using Fourier techniques. CCDC 1875234 ([(**1-Na**)$_8$(NaHMDS)$_2$]), 1875235 (**1H**·LiBr), 1875236 (**1H**), 1875237 ([**1-H$_2$**]Br), 1875238 ([**1-K**·18c6]), 1875239 ([(**1-Li**)$_3$(15c5)]$_2$), 1875240 ([(**1-Li**)$_4$(18c6)]$_\infty$), 1875241 ([(**1-Li**)$_3$(LiHMDS)$_5$]) and 1875242 ([**1-Na**·15c5]) contain the supplementary crystallographic data for this paper. These data can be obtained free of charge from The Cambridge Crystallographic Data Centre. Further information including details to the structure solutions of disorderd parts and solvent molecules is provided in the Supporting Information.

NMR spectroscopy

^{1}H, ^{13}C{^{1}H}, and ^{31}P{^{1}H} NMR spectra were recorded on Avance-400 or DPX-250 spectrometers at 25 °C if not stated otherwise. All values of the chemical shift are in ppm regarding the δ-scale. All spin-spin coupling constants (*J*) are printed in Hertz (Hz). To display multiplicities and signal forms correctly the following abbreviations were used: s = singlet, d = doublet, t = triplet, m = multiplet, br = broad signal. Signal assignment was supported by DEPT, APT, HSQC and HMBC experiments and by literature studies on similar compounds.[8] NMR spectra of all compounds are depicted in the Supporting Information.

Vibrational spectroscopy

IR spectra were recorded on a Thermo Nicolet iS5 FT-IR in transmission mode with a Specac "Omni-cell" with KBr plates and a 0.1 mm spacer at 22 °C. The samples were measured according to standardized procedure: 5 mg of the substance were dissolved in 1 mL of THF in a glovebox (in case of the crown ether complexes 1 equiv of crown ether was added). The solution was added into the IR cell using a syringe. The cell was closed, taken outside the glovebox and an IR spectrum was recorded.

Computational studies

Geometry optimizations without symmetry constraints were carried out with the Gaussian09 program package[35,36] at the B3LYP[37]/6-31+G*[38] level of theory. Initial structures were obtained by using

GaussView 5.0.9.[39] Stationary points were characterized as minima by calculating the Hessian matrix analytically at this level of theory.[40] Thermodynamic corrections and Kohn–Sham orbitals were taken from these calculations. The standard state for all thermodynamic data is 298.15 K and 1 atm. Single-point energies at the B3LYP/6-31+G* optimized geometries were calculated at the B3LYP/6-311++G** level. The NBO[41] analyses were carried out with the internal module of Gaussian09[42] at the B3LYP/6-31+G* level of theory. Coordinates of all optimized structures are given in the Supporting Information.

The EDA-NOCV calculations were carried out with the program package ADF2017.111.[43] The B3LYP/6-31+G* geometries were used. BP86[44] was chosen with uncontracted Slater type orbitals (STOs) as basis functions.[45] The latter basis sets for all elements have triple-ζ quality augmented by two sets of polarization functions (ADF basis set TZ2P). Core electrons (i.e., 1s for second- and [He]2s2p for third-row atoms) were treated by the frozen-core approximation. This level of theory is denoted BP86/TZ2P. An auxiliary set of s, p, d, f and g STOs was used to fit the molecular densities and to represent the Coulomb and exchange potentials accurately in each SCF cycle.[46] Scalar relativistic effects were incorporated by applying the zeroth-order regular approximation (ZORA) in all ADF calculations.[47] The interatomic interactions were investigated by means of an energy-decomposition analysis (EDA) developed independently by Morokuma[48] and by Ziegler and Rauk[49] in conjunction with the natural orbitals for chemical valence (NOCV).[29,50] Further details are provided in the Supporting Information.

Acknowledgements

We thank Prof. Dr. Gernot Frenking for helpful discussions. This project was funded by the European Research Council (ERC) under the European Union's Horizon 2020 research and innovation programme (grant agreement No. 677749) and by the Deutsche Forschungsgemeinschaft (DFG, German Research Foundation) under Germany's Excellence Strategy–EXC-2033–Projektnummer 390677874. We also thank Albemarle (Rockwood Lithium GmbH) for the supply of chemicals.

Conflict of interest

The authors declare no conflict of interest.

Keywords: alkali metals · bond theory · lithium · structure elucidation · solid-state structures · ylides

[1] *Modern Ylide Chemistry: Applications in Ligand Design, Organic and Catalytic Transformations, Structure and Bonding* (Ed.: V. H. Gessner) Springer, Heidelberg, **2018**.

[2] For examples, see: a) A. Fürstner, M. Alcarazo, K. Radkowski, C. W. Lehmann, *Angew. Chem. Int. Ed.* **2008**, *47*, 8302; *Angew. Chem.* **2008**, *120*, 8426; b) S. Khan, G. Gopakumar, W. Thiel, M. Alcarazo, *Angew. Chem. Int. Ed.* **2013**, *52*, 5644; *Angew. Chem.* **2013**, *125*, 5755; c) M. Q. Y. Tay, Y. Lu, R. Ganguly, D. Vidovic, *Angew. Chem. Int. Ed.* **2013**, *52*, 3132; *Angew. Chem.* **2013**, *125*, 3214; d) W. Petz, C. Kutschera, M. Heitbaum, G. Frenking, R. Tonner, B. Neumüller, *Inorg. Chem.* **2005**, *44*, 1263; e) B. Inés, M. Patil, J. Carreras, R. Goddard, W. Thiel, M. Alcarazo, *Angew. Chem. Int. Ed.* **2011**, *50*, 8400; *Angew. Chem.* **2011**, *123*, 8550; f) W. Petz, F. Öxler, B. Neumüller, R. Tonner, G. Frenking, *Eur. J. Inorg. Chem.* **2009**, 4507.

[3] a) W.-C. Chen, J.-S. Shen, T. Jurca, C.-J. Peng, Y.-H. Lin, X.-P. Wang, W.-C. Shih, G. P. A. Yap, T.-G. Ong, *Angew. Chem. Int. Ed.* **2015**, *54*, 15207; *Angew. Chem.* **2015**, *127*, 15422; b) W. Petz, F. Öxler, B. Neumüller, *J. Organomet. Chem.* **2009**, *694*, 4094; c) S. Marrot, T. Kato, H. Gornitzka, A. Baceiredo, *Angew. Chem. Int. Ed.* **2006**, *45*, 2598; *Angew. Chem.* **2006**, *118*, 2660; d) S. Marrot, T. Kato, F. P. Cossio, H. Gornitzka, A. Baceiredo, *Angew. Chem. Int. Ed.* **2006**, *45*, 7447; *Angew. Chem.* **2006**, *118*, 7607; e) J. S. Marcum, C. C. Roberts, R. S. Manan, T. N. Cervarich, S. J. Meek, *J. Am. Chem. Soc.* **2017**, *139*, 15580.

[4] For a discussion about dative bonds in main group element chemistry, see: a) G. Frenking, *Angew. Chem. Int. Ed.* **2014**, *53*, 6040; *Angew. Chem.* **2014**, *126*, 6152; b) D. Himmel, I. Krossing, A. Schnepf, *Angew. Chem. Int. Ed.* **2014**, *53*, 370; *Angew. Chem.* **2014**, *126*, 378; c) D. Himmel, I. Krossing, A. Schnepf, *Angew. Chem. Int. Ed.* **2014**, *53*, 6047; *Angew. Chem.* **2014**, *126*, 6159; d) H. Schmidbaur, *Angew. Chem. Int. Ed.* **2007**, *46*, 2984; *Angew. Chem.* **2007**, *119*, 3042.

[5] a) R. Tonner, F. Öxler, B. Neumüller, W. Petz, G. Frenking, *Angew. Chem. Int. Ed.* **2006**, *45*, 8038; *Angew. Chem.* **2006**, *118*, 8206; b) R. Tonner, G. Frenking, *Chem. Eur. J.* **2008**, *14*, 3260; c) R. Tonner, G. Frenking, *Chem. Eur. J.* **2008**, *14*, 3273; d) R. Tonner, G. Frenking, *Pure Appl. Chem.* **2009**, *81*, 597; e) S. Klein, R. Tonner, G. Frenking, *Chem. Eur. J.* **2010**, *16*, 10160.

[6] a) C. A. Dyker, G. Bertrand, *Nat. Chem.* **2009**, *1*, 265; b) M. Alcarazo, C. W. Lehmann, A. Anoop, W. Thiel, A. Fürstner, *Nat. Chem.* **2009**, *1*, 295.

[7] For reviews, see: a) L. T. Scharf, V. H. Gessner, *Inorg. Chem.* **2017**, *56*, 8599; b) see also ref. [1].

[8] T. Scherpf, R. Wirth, K.-S. Feichtner, S. Molitor, V. H. Gessner, *Angew. Chem. Int. Ed.* **2015**, *54*, 8542; *Angew. Chem.* **2015**, *127*, 8662.

[9] a) T. Scherpf, K.-S. Feichtner, S. Molitor, V. H. Gessner, *Angew. Chem. Int. Ed.* **2017**, *56*, 3275; *Angew. Chem.* **2017**, *129*, 3323; b) T. Scherpf, C. Schwarz, L. T. Scharf, J.-A. Zur, A. Helbig, V. H. Gessner, *Angew. Chem. Int. Ed.* **2018**, *57*, 12859; *Angew. Chem.* **2018**, *130*, 13041; c) P. Weber, T. Scherpf, I. Rodstein, D. Lichte, L. T. Scharf, L. J. Gooßen, V. H. Gessner, *Angew. Chem. Int. Ed.* **2019**; DOI: https://doi.org/10.1002/anie.201810696; *Angew. Chem.* **2019**; DOI: https://doi.org/10.1002/ange.201810696.

[10] a) S. Goumri-Magnet, H. Gornitzka, A. Baceiredo, G. Bertrand, *Angew. Chem. Int. Ed.* **1999**, *38*, 678; *Angew. Chem.* **1999**, *111*, 710; b) T. Baumgartner, B. Schinkels, D. Gudat, M. Nieger, E. Niecke, *J. Am. Chem. Soc.* **1997**, *119*, 12410; c) A. Garduno-Alva, R. Lenk, Y. Escudié, M. L. González, L. Bousquet, N. Saffon-Merceron, C. A. Toledano, X. Bagan, V. Branchadell, E. Maerten, A. Baceiredo, *Eur. J. Inorg. Chem.* **2017**, 3494–3497.

[11] X. Yang, F. F. Fleming, *Acc. Chem. Res.* **2017**, *50*, 2556.

[12] a) X. Yang, D. Natha, F. F. Fleming, *Org. Lett.* **2015**, *17*, 4906; b) F. F. Fleming, Y. Wie, W. Liu, Z. Zhang, *Org. Lett.* **2007**, *9*, 2733; c) F. F. Fleming, Z. Zhang, W. Liu, P. Knochel, *J. Org. Chem.* **2005**, *70*, 2200.

[13] a) H. J. Bestmann, M. Schmidt, *Angew. Chem. Int. Ed. Engl.* **1987**, *26*, 79–81; *Angew. Chem.* **1987**, *99*, 64–65; b) H. J. Bestmann, M. Schmidt, *Tetrahedron Lett.* **1987**, *28*, 2111.

[14] a) J. Vicente, M. T. Chicote, M. C. Lagunas, *Helv. Chim. Acta* **1999**, *82*, 1202; b) A. Johnson, I. Marzo, M. C. Gimeno, *Chem. Eur. J.* **2018**, *24*, 11693.

[15] H. Schmidbaur, A. Schier, *Angew. Chem. Int. Ed.* **2013**, *52*, 176; *Angew. Chem.* **2013**, *125*, 187.

[16] L. T. Scharf, D. M. Andrada, G. Frenking, V. H. Gessner, *Chem. Eur. J.* **2017**, *23*, 4422.

[17] Note that the C=P double bond does not involve a contribution of the d orbitals of phosphorus but population of a σ* orbital of the P–C_{Ph} bond. The central carbon atom exhibits a quintet state $2s^1 2p(\sigma)^1 2p(\pi)^1 2p(\pi')^1$.

[18] For metalation of THF, see: a) A. R. Kennedy, J. Klett, R. E. Mulvey, D. S. Wright, *Science* **2009**, *326*, 706; b) E. Crosbie, P. García-Álvarez, A. R. Kennedy, J. Klett, R. E. Mulvey, S. D. Robertson, *Angew. Chem. Int. Ed.* **2010**, *49*, 9388; *Angew. Chem.* **2010**, *122*, 9578; c) R. E. Mulvey, V. L. Blair, W. Clegg, A. R. Kennedy, J. Klett, L. Russo, *Nat. Chem.* **2010**, *2*, 588; d) A. Maercker, *Angew. Chem. Int. Ed. Engl.* **1987**, *26*, 972; *Angew. Chem.* **1987**, *99*, 1002.

[19] L. B. Krivdin, *Prog. Nucl. Magn. Reson. Spectrosc.* **2018**, *108*, 17.

[20] F. F. Fleming, G. Wei, *J. Org. Chem.* **2009**, *74*, 3551.

[21] M. Purzycki, W. Liu, G. Hilmersson, F. F. Fleming, *Chem. Commun.* **2013**, *49*, 4700.

[22] a) G. Boche, M. Marsch, K. Harms, *Angew. Chem. Int. Ed. Engl.* **1986**, *25*, 373; *Angew. Chem.* **1986**, *98*, 373.

[23] a) R. West, G. A. Gornowicz, *J. Am. Chem. Soc.* **1971**, *93*, 1714.

[24] a) R. Neufeld, R. Michel, R. Herbst-Irmer, R. Schöne, D. Stalke, *Chem. Eur. J.* **2016**, *22*, 12340; b) G. C. Forbes, A. R. Kennedy, R. E. Mulvey, P. J. A. Rodger, *Chem. Commun.* **2001**, 1400; c) M. Karl, G. Seybert, W. Massa, K. Harms, S. Agarwal, R. Maleika, W. Stelter, A. Greiner, W. H. B. Neumüller, K. Dehnicke, *Z. Anorg. Allg. Chem.* **1999**, *625*, 1301; d) F. T. Edelmann, F. Pauer, M. Wedler, D. Stalke, *Inorg. Chem.* **1992**, *31*, 4143; e) N. M. Clark, P. Garcia-Alvarez, A. R. Kennedy, C. T. O'Hara, G. M. Robertson, *Chem. Commun.* **2009**, 5835; f) P. P. Power, X. Xiaojie, *J. Chem. Soc. Chem. Commun.* **1984**, 358; g) K. W. Henderson, A. E. Dorigo, Q.-Y. Liu, P. G. Williard, *J. Am. Chem. Soc.* **1997**, *119*, 11855.

[25] The crystals of $[(\mathbf{1\text{-}Li})_3{\cdot}(15c5)]_2$ were only of poor quality, therefore no bond lengths and angles are discussed here.

[26] a) L. Braun, G. Kehr, T. Blömker, R. Fröhlich, G. Erker, *Eur. J. Inorg. Chem.* **2007**, 3083; b) G. Boche, *Angew. Chem. Int. Ed. Engl.* **1989**, *28*, 277 – 297; *Angew. Chem.* **1989**, *101*, 286 – 306; and references therein.

[27] a) H. Viebrock, T. Panther, U. Behrens, E. Weiss, *J. Organomet. Chem.* **1995**, *491*, 19; b) Y. Liu, T. C. Stringfellow, D. Ballweg, I. A. Guzei, R. West, *J. Am. Chem. Soc.* **2002**, *124*, 49; c) B. Conway, D. V. Graham, E. Hevia, A. R. Kennedy, J. Klett, R. E. Mulvey, *Chem. Commun.* **2008**, 2638; d) W. Clegg, B. Conway, D. V. Graham, E. Hevia, A. R. Kennedy, R. E. Mulvey, L. Russo, D. S. Wright, *Chem. Eur. J.* **2009**, *15*, 7074; e) N. D. R. Barnett, W. Clegg, A. R. Kennedy, R. E. Mulvey, S. Weatherstone, *Chem. Commun.* **2005**, 375.

[28] a) S. P. Green, C. Jones, K.-A. Lippert, D. P. Mills, A. Stasch, *Inorg. Chem.* **2006**, *45*, 7242; b) K. Izod, J. M. Watson, W. Clegg, R. W. Harrington, *Inorg. Chem.* **2013**, *52*, 1466; c) P. García-Álvarez, A. R. Kennedy, C. T. O'Hara, K. Reilly, G. M. Robertson, *Dalton Trans.* **2011**, *40*, 5332.

[29] a) M. Mitoraj, A. Michalak, *Organometallics* **2007**, *26*, 6576; b) M. P. Mitoraj, A. Michalak, T. Ziegler, *J. Chem. Theory Comput.* **2009**, *5*, 962.

[30] A. Krapp, K. K. Pandey, G. Frenking, *J. Am. Chem. Soc.* **2007**, *129*, 7596.

[31] A. J. Lupinetti, S. Fau, G. Frenking, S. H. Strauss, *J. Phys. Chem. A* **1997**, *101*, 9551.

[32] For examples, see: a) R. Luisi, V. Capriati, S. Florio, B. Musio, *Org. Lett.* **2007**, *9*, 1263; b) R. Marcos, L. Xue, R. Sánchez-de-Armas, M. S. G. Ahlquist, *ACS Catal.* **2016**, *6*, 2923; c) A. Causero, G. Ballmann, J. Pahl, C. Färber, J. Intemann, S. Harder, *Dalton Trans.* **2017**, *46*, 1822; d) J. M. Asensio, R. Andrés, P. Gómez-Sal, E. de Jesús, *Organometallics* **2017**, *36*, 4191; e) J. E. Heimann, W. H. Bernskoetter, N. Hazari, J. M. Mayer, *Chem. Sci.* **2018**, *9*, 6629.

[33] G. P. Schiemenz, H. Engelhard, *Chem. Ber.* **1961**, *94*, 578 – 585.

[34] a) G. M. Sheldrick, *Acta Crystallogr. Sect. A* **2008**, *64*, 112; b) A. Thorn, B. Dittrich, G. M. Sheldrick, *Acta Crystallogr. Sect. A* **2012**, *68*, 448; c) G. M. Sheldrick, *Acta Crystallogr. Sect. C* **2015**, *71*, 3.

[35] C. Peng, P. Y. Ayala, H. B. Schlegel, M. J. Frisch, *J. Comput. Chem.* **1996**, *17*, 49.

[36] Gaussian 09 (Revision E.01), M. J. Frisch, G. W. Trucks, H. B. Schlegel, G. E. Scuseria, M. A. Robb, J. R. Cheeseman, G. Scalmani, V. Barone, B. Mennucci, G. A. Petersson, H. Nakatsuji, M. Caricato, X. Li, H. P. Hratchian, A. F. Izmaylov, J. Bloino, G. Zheng, J. L. Sonnenberg, M. Hada, M. Ehara, K. Toyota, R. Fukuda, J. Hasegawa, M. Ishida, T. Nakajima, Y. Honda, O. Kitao, H. Nakai, T. Vreven, J. A. Montgomery, Jr., J. E. Peralta, F. Ogliaro, M. Bearpark, J. J. Heyd, E. Brothers, K. N. Kudin, V. N. Staroverov, R. Kobayashi, J. Normand, K. Raghavachari, A. Rendell, J. C. Burant, S. S. Iyengar, J. Tomasi, M. Cossi, N. Rega, J. M. Millam, M. Klene, J. E. Knox, J. B. Cross, V. Bakken, C. Adamo, J. Jaramillo, R. Gomperts, R. E. Stratmann, O. Yazyev, A. J. Austin, R. Cammi, C. Pomelli, J. W. Ochterski, R. L. Martin, K. Morokuma, V. G. Zakrzewski, G. A. Voth, P. Salvador, J. J. Dannenberg, S. Dapprich, A. D. Daniels, Ö. Farkas, J. B. Foresman, J. V. Ortiz, J. Cioslowski, D. J. Fox, Gaussian, Inc., Wallingford CT, **2009**.

[37] a) A. D. Becke, *J. Chem. Phys.* **1993**, *98*, 5648; b) C. Lee, W. Yang, R. G. Parr, *Phys. Rev. B* **1988**, *37*, 785; c) S. H. Vosko, L. Wilk, M. Nusair, *Can. J. Phys.* **1980**, *58*, 1200; d) P. J. Stephens, F. J. Devlin, C. F. Chabalowski, M. J. Frisch, *J. Phys. Chem.* **1994**, *98*, 11623.

[38] a) A. D. McLean, G. S. Chandler, *J. Chem. Phys.* **1980**, *72*, 5639; b) K. Raghavachari, J. S. Binkley, R. Seeger, J. A. Pople, *J. Chem. Phys.* **1980**, *72*, 650.

[39] R. Dennington, T. Keith, J. Millam 2009 GaussView, Version5.0.9 (Shawnee Mission, KS: Semichem Inc.).

[40] P. Deglmann, F. Furche, R. Ahlrichs, *Chem. Phys. Lett.* **2002**, *362*, 511.

[41] A. E. Reed, L. A. Curtiss, F. Weinhold, *Chem. Rev.* **1988**, *88*, 899.

[42] NBO Version 3.1, E. D. Glendening, A. E. Reed, J. E. Carpenter, F. Weinhold.

[43] a) F. Bickelhaupt, E. J. Baerends in *Reviews in Computational Chemistry, Vol. 15*, Wiley, New York, **2000**, p. 1; b) G. te Velde, F. M. Bickelhaupt, E. J. Baerends, C. F. Guerra, S. D. J. A. Van Gisbergen, J. Snijders, T. Ziegler, *J. Comput. Chem.* **2001**, *22*, 931; c) ADF2013, SCM, Theoretical Chemistry, Vrije Universiteit, Amsterdam, The Netherlands, http://www.scm.com.

[44] a) A. D. Becke, *Phys. Rev. A* **1988**, *38*, 3098; b) J. P. Perdew, *Phys. Rev. B* **1986**, *33*, 8822.

[45] J. G. Snijders, P. Vernoojs, E. J. Baerends, *At. Data Nucl. Data Tables* **1981**, *26*, 483; E. Van Lenthe, E. J. Baerends, *J. Comput. Chem.* **2003**, *24*, 1142.

[46] J. Krijn, E. Baerends, Fit Functions in the HFS-Method, Internal Repot (in Dutch), Vrije Universiteit Amsterdam, The Netherlands, **1984**.

[47] a) E. Van Lenthe, E. J. Baerends, J. G. Snijders, *J. Chem. Phys.* **1993**, *99*, 4597; b) E. Van Lenthe, E. J. Baerends, J. G. Snijders, *J. Chem. Phys.* **1994**, *101*, 9783; c) E. Van Lenthe, A. Ehlers, E. J. Baerends, *J. Chem. Phys.* **1999**, *110*, 8943.

[48] K. Morokuma, *J. Chem. Phys.* **1971**, *55*, 1236.

[49] a) T. Ziegler, A. Rauk, *Inorg. Chem.* **1979**, *18*, 1755; b) T. Ziegler, A. Rauk, *Inorg. Chem.* **1979**, *18*, 1558.

[50] a) M. Mitoraj, A. Michalak, *J. Mol. Model.* **2007**, *13*, 347; b) A. Michalak, M. Mitoraj, T. J. Ziegler, *J. Phys. Chem. A* **2008**, *112*, 1933; c) M. Mitoraj, A. Michalak, *J. Mol. Model.* **2008**, *14*, 861.

Manuscript received: October 30, 2018

Accepted manuscript online: December 17, 2018

Version of record online: January 29, 2019

